Acousto-optic imaging of a color picture hidden behind a scattering layer

Terence S. Leung[1,*] and Shihong Jiang[1]

[1]Department of Medical Physics and Bioengineering, Malet Place Engineering Building, University College London, London, WC1E 6BT, UK
[*]t.leung@ucl.ac.uk

Abstract: An imaging technique has been developed to image a color picture hidden behind a 5 mm thick, highly scattering layer with low transmittance of 0.24%. Small vibrations (< 1 μm) were induced in the hidden picture, causing a time-varying speckle pattern on the scattering layer in the front, which is captured by a CCD camera and quantified as speckle contrast difference (SCD). With two lasers at 543 nm and 633 nm, the imaging system raster-scans the front of the scattering layer and the resulting SCD image reveals the color features of the hidden picture.

References and links

1. O. Katz, E. Small, and Y. Silberberg, "Looking around corners and through thin turbid layers in real time with scattered incoherent light," Nat. Photonics **6**, 549-553 (2012).
2. A. P. Mosk, A. Lagendijk, G. Lerosey, and M. Fink, "Controlling waves in space and time for imaging and focusing in complex media," Nat. Photonics **6**, 283-292 (2012).
3. I. M. Vellekoop and A. P. Mosk, "Focusing coherent light through opaque strongly scattering media," Opt. Lett. **32**, 2309-2311 (2007).
4. J. Bertolotti, E. G. Van Putten, C. Blum, A. Lagendijk, W. L. Vos, and A. P. Mosk, "Non-invasive imaging through opaque scattering layers," Nature **491**, 232-234 (2012).
5. T. S. Leung and S. Jiang, "Classifying hidden colors behind an opaque layer with the acoustically modulated laser speckle contrast technique," Opt. Express **21**, 20197-20209 (2013).
6. M. Draijer, E. Hondebrink, T. Van Leeuwen, and W. Steenbergen, "Review of laser speckle contrast techniques for visualizing tissue perfusion," Laser Med Sci **24**, 639-651 (2009).
7. S. M. Bentzen, "Evaluation of the spatial resolution of a CT scanner by direct analysis of the edge response function," Med Phys **10**, 579-581 (1983).
8. S. Lloyd-Fox, A. Blasi, and C. E. Elwell, "Illuminating the developing brain: The past, present and future of functional near infrared spectroscopy," Neurosci Biobehav R **34**, 269-284 (2010).
9. G. T. Clement and K. Hynynen, "A non-invasive method for focusing ultrasound through the human skull," Phys. Med. Biol. **47**, 1219-1236 (2002).

1. Introduction

When light propagates through a highly scattering medium, it loses its directionality and most of its spatial information. An object hidden behind a scattering medium, e.g., a frosted glass, will therefore appear blurry to the naked eyes and its exact shape can no longer be identified. However, the recent development of the spatial light modulator technology, which allows the shaping of the wavefront of light, has been demonstrated to be capable of focusing diffuse light through a scattering medium and even recovering the image hidden behind it [1-3]. Instead of using a spatial light modulator, another recent study exploited the relationship between the light beam's incident angle and the total fluorescence (the memory effect), and used an iterative algorithm to reconstruct a hidden fluorescent image [4]. The scattering media used in these studies are often materials with high transmittance (>75%) such as polycarbonate or ground-glass diffusers. Although potentially feasible, these techniques have

yet to be shown to work in scattering media with low transmittance (<1%), which would be the case for deep tissue imaging, one of the major target applications of these techniques. In this work, we demonstrate an acousto-optic technique, known as the acoustically modulated laser speckle contrast (AMLSC) technique [5], that can recover a color image hidden behind a scattering layer with transmittance as low as 0.24%, in a reflection configuration. The new imaging capability allows color features hidden beneath a superficial layer to be estimated in two dimensions, greatly improving its functionality in biomedical applications, e.g. it can potentially locate and size subdural hematomas beneath the skull in head injured patients.

2. Methods

2.1 Theory

In the previous technique [5], a single-color paper, hidden behind a scattering layer, was subject to small-amplitude vibrations. A coherent laser illuminated the front of the scattering layer, producing a speckle pattern. Two types of light contribute to the formation of the speckle pattern: (i) I_b, the background light that has only interacted with the scattering layer and reflected back, and (ii) I_m, the light that has propagated through the scattering layer, reached the color paper, modulated by its small vibration and reflected back.

Without the vibration, the media (the scattering layer and color paper) are static and so is the speckle pattern. With the vibration at the color paper, however, the media become dynamic and the speckle pattern varies spatially over time. Because of the motion artifact, the speckle image captured by a CCD camera becomes blurry. To some degree, the "blurriness" can indicate the absorption (color) of the hidden object, e.g., if the hidden object is highly absorbing (black) and all the light that reaches it has been absorbed ($I_m = 0$), the speckle pattern would still be static even when the black color paper is vibrating. Subsequently, the speckle image is no longer blurry. The blurriness can be quantified by calculating the speckle contrast of the speckle image, defined as $C = \sigma / <I>$ where σ and $<I>$ are the standard deviation and mean of all the pixel intensity of the speckle image [6]. It can be shown that the speckle contrast difference, defined as $\Delta C = C_{off} - C_{on}$, can be approximated as [5]:

$$\Delta C \approx \frac{\sqrt{C_b^{\,2} + 2M} - C_b}{1 + M} \tag{1}$$

where $C_b = \sqrt{\langle I_b^2 \rangle - \langle I_b \rangle^2} / \langle I_b \rangle$ and $M = \langle I_m \rangle / \langle I_b \rangle$.

It has been shown previously from Eq. (1) that ΔC increases monotonically with $<I_m>$ while $<I_b>$ is kept constant [5]. Since $<I_m>$ is determined by the absorption (color) of the hidden object, ΔC carries information about the color of the hidden object, allowing the color of the object to be "seen" through the opaque, highly scattering medium.

In the current work, instead of a single-color paper, a multi-color picture (red, green, blue, white and black) has been hidden behind a highly scattering layer. Rather than vibrating the whole color paper as before, the color picture is locally vibrated by a small hammer (a 2 mm screw). The scattering layer and the hidden color picture were raster-scanned, and the ΔC at each scanned position forms the value of a pixel on the resulting image. For comparison, images were also formed using the mean pixel intensity (pure optical technique).

In general, a color object reflects more light of the same color, e.g., a red object would reflect more red light and absorbs more, say, green light. (A white object reflects all colors of light equally well.) In order to recover the red, green and white features of the hidden picture, two lasers (green and red) have been used in this work.

2.2 Experimental setup

Fig. 1 depicts the current experimental setup of the AMLSC technique which is similar to that of the previous work [5]. An opaque, highly scattering layer (the photo in Fig. 1), which was made of epoxy resin with a thickness of 5 mm, reduced scattering coefficient $\mu_s'(633 \text{ nm}) =$

1.8 mm^{-1}, absorption coefficient μ_a(780 nm) = 0.01 mm^{-1} and 0.24% transmittance, was securely fixed to the optical table. A color picture (40 mm × 40 mm), which acted as a light reflector, was placed behind the scattering layer, secured by a paper frame leaving a 1 mm air gap in between. A 2 mm screw, which was attached to the center of the loudspeaker's diaphragm, acted as a small hammer hitting the color picture slightly to generate a localized vibration. The vibration amplitude was small (< 1 µm as measured by a laser sensor, Micro-Epsilon ILD1700-10) and the scattering layer practically experienced no vibration. The loudspeaker was driven by a function generator (33210A, Agilent) at 200Hz.

Two He-Ne lasers, i.e. green (wavelength λ = 543 nm, 1 mW, beam diameter = 0.86 mm, Melles Griot) and red (λ = 633 nm, 10 mW, beam diameter = 0.68 mm, Melles Griot), were employed as the light sources and a CCD camera (ORCA-03G, Hamamatsu Photonics KK.) as the detector. A lens with a 100 mm focal length and a 10 mm diameter iris gave a *f* number (*f*/#) of 10. A magnification factor (M) of 2× was chosen to produce a field of view of 4.3 × 3.3 mm. The distance between the entry point of the laser beam and the center of the sensor's field of view was 5 mm. A 45° reflective green dichroic filter (#47-265, Edmund Optics) was used which allowed red light to transmit and green light to reflect. The red and green lasers were used in turn. A neutral density filter was placed in front of the CCD camera to allow the flexibility to change the exposure time under different illumination conditions without saturating the detector pixels. The exposure time of the CCD camera was set to 0.1/0.5 ms for the red/green laser. The experiment was conducted in a black enclosure for eye safety reason. The AMLSC technique is in general insensitive to non-coherent light such as ambient light although excessive ambient light may saturate the CCD detectors, affecting the performance.
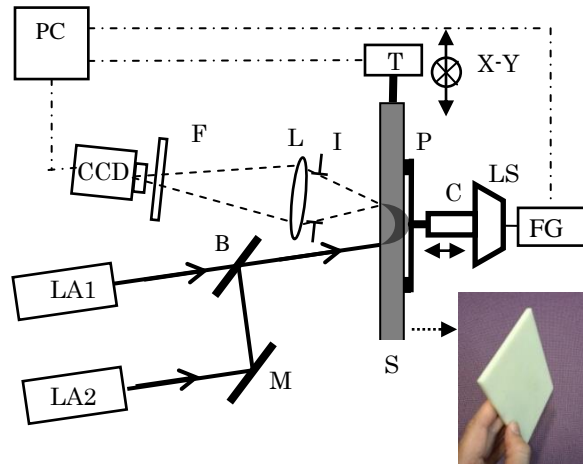

Fig.1 Experimental setup: LA1 – red laser; LA2 – green laser; B – dichroic filter ; M – mirror; I – iris; L – lens; S – scattering layer; P – color picture; C – connecting rod with a 2 mm screw at the tip; LS – loudspeaker; FG – function generator; F – Neutral density filter; CCD – CCD camera, T – 2-axes translation stage, PC – computer, and a photo of the scattering layer
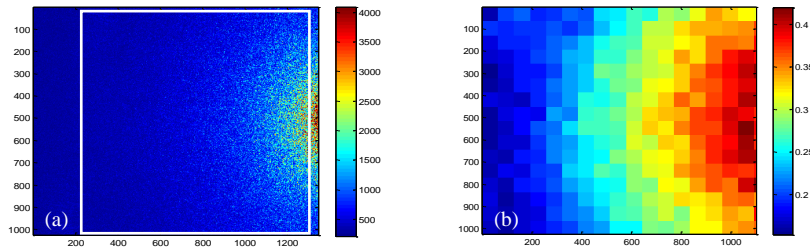

Fig.2 Speckle image: (a) the original speckle intensity image (1344×1024 pixels = 4.3×3.3 mm), part of it (white box) cropped for analysis; (b) the cropped speckle contrast C (= σ / <I>) image (1100×1024 pixels = 3.5×3.3 mm)

The CCD camera produced a 12-bit monochrome image with a dimension of 1344×1024 as shown in Fig. 2(a) which is plotted in a color scale for easy visualization. The field of view was adjusted to capture only part of the beam spot on the surface of the scattering layer to avoid the brightest spot which would otherwise saturate the CCD detectors. At each scan position, 10 images with the sound on and 10 images with the sound off were recorded. The recorded images were cropped to exclude the areas exposed to too much or too little light as shown in Fig. 2(a). The cropped image was divided into tiled rectangular blocks. Each block had a size of 64×64 pixels. The speckle contrast values C were calculated for each block as depicted in Fig. 2(b) and then averaged across all the blocks. Trimmed mean was calculated in the 10 sound-on images (C_{on}) and 10 sound-off images (C_{off}) respectively to exclude outliers, followed by the calculation of $\Delta C = C_{off} - C_{on}$.

3. Results

3.1 Spatial resolution evaluated by the line spread function

Two series of experiments were conducted. In the first one, the line spread function (LSF) was measured to assess the spatial resolution of the AMLSC technique under different conditions. In the second one, the AMLSC technique was employed to image a black-and-white and a color picture hidden behind the scattering layer.

In the first series of experiments, the edge spread function was first measured for a picture consisting of two color rectangles, e.g., black and white, hidden behind the scattering layer. As depicted in Fig. 3(a), the edge spread function was formed by ΔC measured at each scanned position, with position zero corresponding to the boundary (edge) between the black and white rectangles. The scan was repeated 10 times and all the ΔC values were used to fit a model of the edge spread function which can then be converted into a LSF [7]. The LSF is an intuitive and quantitative way to assess the spatial resolution of an imaging technique. In general, the narrower the bell-shaped LSF, the better the spatial resolution.

The result in Fig. 3(a) can be understood by considering I_m in Eq. (1), which is formed by the light that reflects back from the hidden picture and is directly related to ΔC. Due to scattering in the scattering layer, the laser beam is diffuse and its spot size becomes much larger on the surface of the hidden picture. Depending on what colors are present within the "diffuse illuminated spot", I_m (and therefore ΔC) will have different values. For instance, pure white color (reflects more light) will give rise to a larger I_m while pure black color (absorbs more light) a smaller I_m. When both white and black colors are present within the diffuse illuminated spot, I_m will have a value in between, depending on the proportion of each color in the region. This explains the change in ΔC as the raster scan shifts from left (black) to right (white) in Fig. 3(a). In our experiment, the orientation of the laser source and the CCD camera was fixed. Since the speckle contrast image, from which ΔC is calculated, is asymmetrical in the horizontal direction as depicted in Fig. 2(b), the spatial resolution in the horizontal scan direction is different from that in the vertical scan direction. Fig. 3(b) shows the LSF of the vertical scan direction has a slightly better spatial resolution than that of the horizontal scan direction. Next, different combinations of colors were used as the hidden picture.

Figure 3(c) shows that with the red laser as the light source, the LSF of the black/red combination has a similar spatial resolution as the black/white combination, which is expected because the red and white colors reflect similar amount of red light according to our direct reflectance measurements of the two colors without barrier. Fig. 3(d), on the other hand, shows that the LSF of the black/white combination is significantly narrower (better spatial resolution) than the black/green combination, using the green laser as the light source. This is also expected because the white color reflects more green light than the green color does (According to our measurement, the white color has a larger direct reflectance than the green color at 543 nm). In fact, other color combinations were also attempted but very little change in ΔC was found when (i) the red laser was used for the black/blue and black/green combinations, and (ii) the green laser was used for the black/blue and black/red combinations. The colors black, blue and green all have very small direct reflectance at 633 nm and the

colors black, blue and red have equally small direct reflectance at 543 nm. The scattering layer used so far had a thickness of 5 mm. Next, the LSFs for three thicknesses (3, 5 and 8 mm) of the scattering layer were measured with the black/white rectangles as the hidden picture, and the red and green lasers as the light sources, as shown in Fig. 3(e) and (f) respectively. The results show that in both cases, the LSF becomes broader (spatial resolution getting worse) as the thickness of the scattering layer increases. This is because as the thickness increases, higher scattering results in a larger diffuse illuminated spot on the hidden picture, which also means a lower spatial resolution. Theoretically, a larger laser beam size may also lead to a larger diffuse illuminated spot and therefore a lower spatial resolution. In practice, since the light is heavily scattered after propagating through a highly scattering layer, only a substantially larger beam size would cause any visible difference.
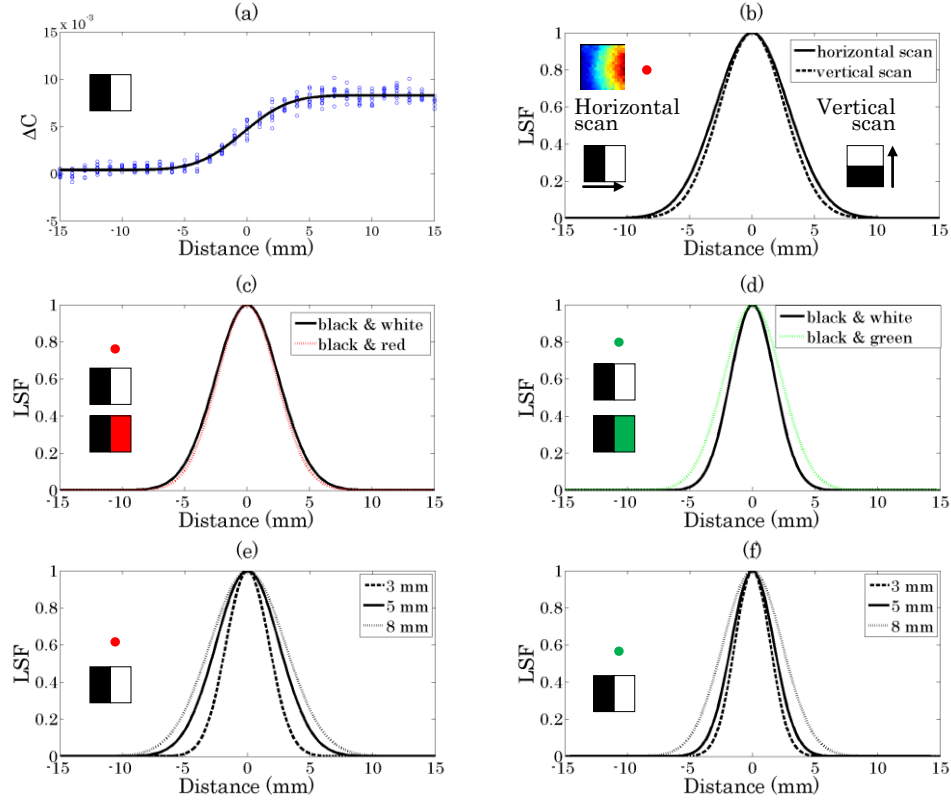

Fig. 3 Spatial resolution assessment: (a) the edge spread function, inset is the color picture hidden behind the scattering layer; (b) the line spread function (LSF) of the horizontal and vertical scans; the LSFs of the hidden pictures with different color combinations using (c) the red laser and (d) the green laser; the LSFs for different thicknesses of the scattering layers using (e) the red laser and (f) the green laser. (Insets are the hidden color pictures.)

3.2 Imaging of hidden color pictures

In the second series of experiments, two hidden pictures were imaged. For a better visualization, the resulting images were interpolated, increasing the total number of pixels by a factor of 15. As shown in Fig. 4(b), the first hidden image was a black and white character "A". Using red laser illumination, the intensity image depicted in Fig. 4(a) does not show anything at all. The "black patch" located in the middle lower half was found to be a faint pencil marking on the surface of the scattering layer. The ΔC image in Fig. 4(c), on the other hand, shows the outline of the character "A", and no black patch can be found, showing the approach is independent of color change on the scattering layer.

Figure 4(e) shows the second hidden image which is a color picture consisting of four color blocks: red, green, blue and white. Figs. 4(g) and 4(h) depict the intensity images with red and green laser illumination, respectively. Again, very little information about the hidden image can be revealed by these images. The red and green images were combined to form a multicolor picture by assigning them as the red and green parts of a RGB image while the blue part was all set to zero. Fig. 4(d) is the combined intensity RGB image which again does not reveal any meaningful feature of the hidden picture.

Figures 4(i) and 4(j) are the ΔC images using the red and green laser illumination, respectively. The red and white blocks can be seen from Fig. 4(i) while the green and white blocks are evident in Fig. 4(j). By combining the two images using a similar approach as described in the last paragraph, a combined ΔC RGB image is formed as depicted in Fig. 4(f) which reveals a color image with the red, green and white blocks. The blue block cannot be identified because the blue color absorbs a relatively large amount of red and green light, as mentioned earlier during the discussion of Figs. 3(c) and 3(d) in section 3.1. However, with an additional laser, e.g., a blue laser, which is less absorbed by the blue color, the AMLSC technique should be able to reveal also the blue block in this color picture.
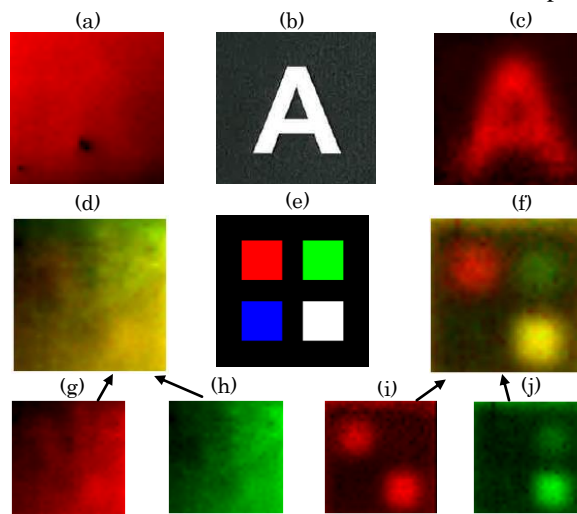

Fig. 4 Hidden pictures and imaging results, (I): character 'A' as the hidden picture using the red laser – (a) the intensity image, (b) the hidden black and white picture and (c) the ΔC image; and (II) color blocks as the hidden picture using the red and green lasers separately – (d) the combined intensity RGB image, (e) the hidden color picture, (f) the combined ΔC RGB image, (g) the intensity image using the red laser, (h) the intensity image using the green laser, (i) the ΔC image using the red laser, and (j) the ΔC image using the green laser.

4. Conclusion

We have demonstrated that the AMLSC technique can image a color picture hidden behind a highly scattering layer. This capability opens up a range of potential biomedical applications involving mapping color features behind a superficial layer, e.g., mapping oxygenation change over the brain cortex hidden beneath the skull during functional task experiments [8], and mapping the location and size of subdural hematomas beneath the skull in head injured patients. The challenge here is to induce small acoustic modulation in the brain which can potentially be achieved by employing ultrasound [9].

Acknowledgment